

# Northeast Materials Database (NEMAD): Enabling Discovery of High Transition Temperature Magnetic Compounds

Suman Itani<sup>1,\*</sup>, Yibo Zhang<sup>1,2,\*</sup>, and Jiadong Zang<sup>1,\*</sup>

<sup>1</sup>Department of Physics and Astronomy, University of New Hampshire, Durham, 03824, USA

<sup>2</sup>Department of Chemistry, University of New Hampshire, Durham, 03824, USA

\*suman.itani@unh.edu, yibo.zhang@unh.edu, jiadong.zang@unh.edu

## ABSTRACT

The discovery of novel magnetic materials with greater operating temperature ranges and optimized performance is essential for advanced applications. Current data-driven approaches are challenging and limited due to the lack of accurate, comprehensive, and feature-rich databases. This study aims to address this challenge by introducing a new approach that uses Large Language Models (LLMs) to create a comprehensive, experiment-based, magnetic materials database named the Northeast Materials Database (NEMAD), which consists of 26,706 magnetic materials ([www.nemad.org](http://www.nemad.org)). The database incorporates chemical composition, magnetic phase transition temperatures, structural details, and magnetic properties. Enabled by NEMAD, machine learning models were developed to classify materials and predict transition temperatures. Our classification model achieved an accuracy of 90% in categorizing materials as ferromagnetic (FM), antiferromagnetic (AFM), and non-magnetic (NM). The regression models predict Curie (Néel) temperature with a coefficient of determination ( $R^2$ ) of 0.86 (0.85) and a mean absolute error (MAE) of 62K (32K). These models identified 62 (19) FM (AFM) candidates with a predicted Curie (Néel) temperature above 500K (100K) from the Materials Project. This work shows the feasibility of combining LLMs for automated data extraction and machine learning models in accelerating the discovery of magnetic materials.

## Introduction

For centuries, magnetic materials have been discovered and studied due to their broad applications in modern science and technology, including data storage devices, energy technologies, advanced medical equipment, quantum computing, and consumer electronics<sup>1-3</sup>. Searching for efficient magnetic materials is crucial to addressing global energy challenges and revolutionizing the technology industry<sup>4</sup>. For example, high-performance permanent magnets can increase efficiency in renewable energy, like wind power and hydroelectric power generators. At the same time, the consumption of fossil fuels and greenhouse gases is reduced. It can also give us high density data storage solutions. Despite of these wide applications, limits for existing magnetic materials are present. For example, most high-performance magnetic materials contain rare earth elements and have a limited operating temperature range<sup>5,6</sup>. The discovery of novel magnetic materials with greater operating temperature ranges using more abundant elements is a fundamental challenge in material science, partly due to the vast combinatorial space of possible compositions and the limitations of conventional methods.

The conventional techniques for material discovery have been largely based on systematic exploration of compositional space and intuition-directed experimentation. Although successful, these approaches require a lot of time and resources, and they can take years to produce useful outcomes<sup>7</sup>. The development of computational methods has opened up exciting new avenue toward materials discovery and property prediction. The first principles calculation such as the density functional theory (DFT) has enabled the predictions of material properties<sup>8,9</sup>. Exploration of vast compositional spaces has been possible using high-throughput computational screening<sup>10,11</sup>. These computational breakthroughs have resulted in the construction of huge materials databases, such as the Materials Project<sup>10</sup>, AFLOW<sup>11</sup>, AFLOWLIB<sup>12</sup>, and OQMD<sup>13</sup>. Unfortunately, applying DFT to predict the magnetic properties of magnetic materials generally leads to less reliable results. Using the standard exchange-correlation functionals could not accurately describe the strongly correlated electron system in magnetic materials especially itinerant magnets. To accurately describe such a system, one should impose the space and spin symmetry constraints as done in ab initio wave function theory. However, the DFT method could not properly incorporate these constraints<sup>14</sup>. The integration of electronic structure information and mean field models for determining exchange interaction and constructing an effective Hamiltonian is a conventional approach in calculating the Curie temperature<sup>15-18</sup>. This method, however, receives good results only for a short list of materials<sup>19</sup>. Moreover, the requirement for prior knowledge of the crystal structure of

the material also puts a limit on the applicability of the DFT method. Another drawback of DFT calculation is that it is mostly limited to the materials of small unit cells due to the high computational costs of large unit cells<sup>20,21</sup>. Due to the above constraints, determining the magnetic properties and discovering novel magnetic materials remains a difficult task.

The data-driven approach is a new paradigm of research that has received great interest in recent years because of its capabilities in accurate predictions and discovering hidden patterns that otherwise may get missed by traditional methods<sup>22,23</sup>. Machine learning predicts physical properties quickly, discovers new materials, and optimizes the existing ones by analyzing large datasets<sup>24,25</sup>. Specifically, several machine learning models have been developed to classify the magnetic material and predict magnetic properties, including phase transition temperatures and coercivity fields<sup>26-35</sup>. However, the performance of all these machine learning models highly depends on the availability and quality of a comprehensive magnetic materials database, which has not yet been fully available. It is rather challenging to identify trends across different classes of magnetic materials without such a comprehensive database, potentially overlooking promising research directions. For instance, the models were trained on extremely small data points of high-temperature regions specifically for the phase transition temperature prediction<sup>26,31</sup>. This may generate less accurate predictions in that region which in turn undermines the discovery of high transition temperature materials. MAGDATA<sup>36,37</sup> is a manually curated database comprising information for around 2000 magnetic materials with experimentally verified lattice and magnetic structure features. Due to its very modest size of dataset, fewer features, and being designed for single-entry lookups, the implementation of data-driven methods on that is challenging and less effective. Some articles and books have noticed some efforts to create a magnetic material database, but the data are scattered and hard to access electronically and systematically<sup>26,28,38-40</sup>.

With the advent of the natural language processing (NLP), its combination with machine learning makes it possible to generate an automated database of magnetic materials<sup>41</sup>. An automatically generated database using the ChemDataExtractor toolkit and Snowball algorithm shows the power of this technique by including 39,822 records. But the database is restricted to only a few features, such as chemical compositions and their associated magnetic phase transition temperatures, which are relatively easy to extract from articles. This approach was less accurate when extracting information involving multiple materials or when the data came in varied sentence structures. Another study has been done to build an auto-generated database of 3,613 ferromagnetic compounds with their corresponding Curie temperature<sup>42</sup>. They used a method based on fine-tuning bidirectional encoder representations from transformers (BERT) models. The database shows high quality and accuracy, making it valuable for developing machine learning models to predict material properties. However, database size and features are limited, and they failed to extract data from the tables of a scientific article. Nevertheless, the machine learning models built on both auto-generated databases showed encouraging performance, as indicated by the statistical parameters  $R^2$ , MAE, and RMSE.

However, the magnetic properties of the materials strongly depend on the structural details of the material such as crystal structure, lattice structure, lattice parameters, and space group symmetry<sup>43</sup>. Also, for the study of a particular magnetic material such as a permanent magnet, one needs to know the information about magnetization, coercivity, and magnetic anisotropy. All of the existing auto-generated databases lack these important information. Therefore, to make the data-driven method more effective for magnetic material discovery, a comprehensive database with greater features is needed.

Recent advancement of NLP, the large language models (LLMs), enables researchers to quickly and easily interact with a chatbot to extract their desired information in a structured format from a large chunk of unstructured text. Its applications in the field of science and technology are emergent<sup>44-46</sup>. As one important application, the GPTArticleExtractor workflow<sup>47</sup> developed by the authors provides a way to make a comprehensive material property database by automatically extracting data from scientific articles with high precision.

In this work, using the GPTArticleExtractor workflow shown in Figure 1, we have developed a database of 26,706 magnetic materials, incorporating chemical composition, structural details (such as crystal structure, lattice structure, lattice parameters, and space group symmetry), and magnetic properties (such as coercivity, magnetization, magnetic moment, remanence, and susceptibility). We then implemented this database to train machine learning models, including Random Forest (RF) classifier, Random Forest (RF) regressor, Extreme Gradient Boosting (XGBoost), and Ensemble Neural Network (ENN) for classifying magnetic materials and predicting transition temperature (Curie and Néel). The performance of these models were evaluated by cross-validation techniques. Our classification model achieved 90% accuracy in classifying materials as ferromagnetic, antiferromagnetic, or non-magnetic. Our best Curie temperature prediction model with features generated from chemical composition (chemical composition + structure) predicts Curie temperature with an  $R^2$  value of 0.86 (0.86) and a mean absolute error of 62K (52K). Similarly, our best Néel temperature prediction model with features generated from only chemical composition predicts Néel temperature with an  $R^2$  value of 0.85 and a mean absolute error of 32K. This model identified 62 promising ferromagnetic candidates with predicted Curie temperatures exceeding 500K and 19 antiferromagnetic compounds with predicted Néel temperature greater than 100K.

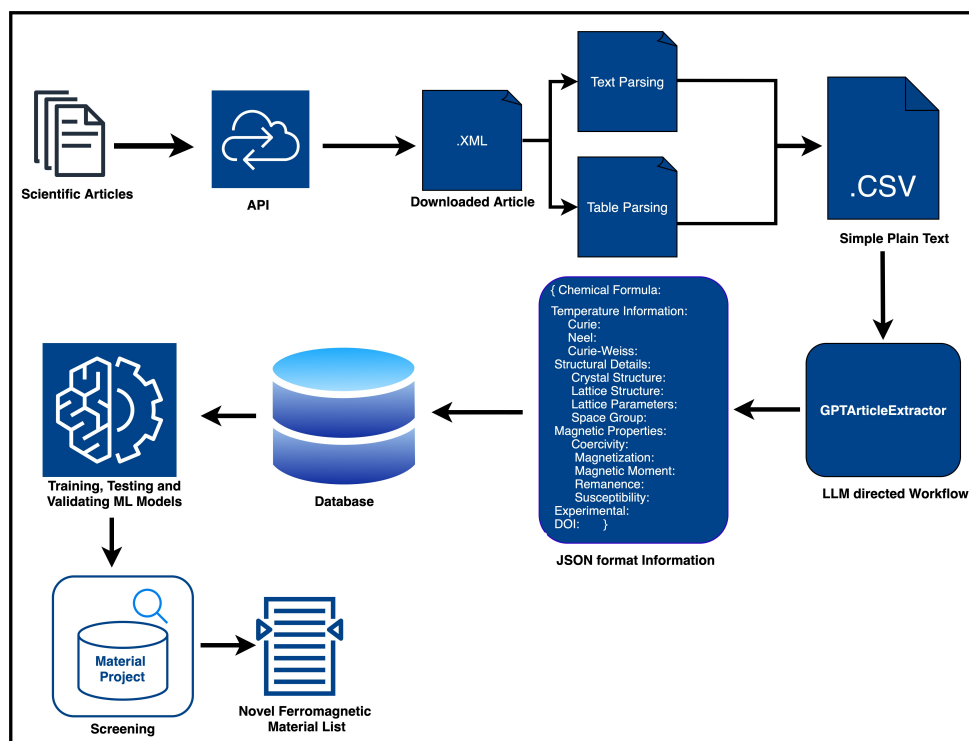


**Figure 1. Workflow for automated magnetic materials database creation and analysis.** This work retrieves DOIs of scientific articles, downloads and parses the XML files, and creates a CSV file. Information extraction is handled by the GPTArticleExtractor model, which uses prompt engineering, text tokenization, and FAISS. It produces a consistent JSON output through one-shot prompting. Next, a database is generated and manually validated. This database is then used to develop machine learning models that classify materials as FM, AFM, or NM and predict Curie and Néel temperatures, ultimately screening for high-performance magnetic compounds in the Materials Project database.

## RESULTS

### NEMAD: A Comprehensive Database of Magnetic Materials

By applying state-of-the-art LLMs to scholarly *experimental* articles published in Elsevier journals, see details in the Methods section, we have constructed the NEMAD database to provide complete and accurate information on magnetic materials and their corresponding properties. The database includes 26,706 magnetic materials, uniquely defined by chemical composition, structural detail, and magnetic properties. Each entry contains fifteen features listed in Table 1. The chemical composition of each magnetic material was collected initially as string data, but was later converted into a numerical format by feature engineering techniques detailed in Methods, making it easy for training machine learning models.

NEMAD includes both ferromagnetic and antiferromagnetic materials identified by their temperature record. Around 65% of the records in the database are ferromagnets. Records with solely Néel temperature classified as antiferromagnets make up about 33% of the database. Only a tiny percentage (about 3%) of materials have both Curie and Néel temperatures due to their complicated phase diagrams. The Curie-Weiss temperature is another feature that contains important information for the magnetic properties. Discrepancy between the Curie-Weiss temperature and transition temperature usually indicates competing interactions in the material. The distributions of Curie and Néel temperatures throughout the database are shown in Figures 2a and 2b. It is noteworthy that almost 22% of the compounds have Curie temperatures higher than 600K, suggesting broad temperature distributions and the possibility of using this database to search high Curie temperature materials.

In addition, the database comprises structural details of the magnetic compounds such as crystal structure, lattice structure, lattice parameters, and space groups. This structural data is necessary for creating advanced machine learning models like graph neural networks. It also provides several magnetic property values in the relevant units, including coercivity, magnetization, magnetic moment, remanence, and susceptibility. These features are useful in data-driven discovery regarding high-performance magnetic materials, particularly permanent magnets.

The elemental composition of the NEMAD database is extensive, including 84 different elements. The frequencies of these

**Table 1.** Description of Features in the NEMAD Database

Column Name	Type	Unit	Description
Material_Chemical_Composition	String		Chemical composition of the magnetic compound
Curie	Numeric	K	Curie temperature value of compound
Néel	Numeric	K	Néel temperature value of compound
Curie Weiss	Numeric	K	Curie Weiss temperature value of compound
Crystal Structure	String		Crystal structure of compound
Lattice Structure	String		Lattice structure of compound
Lattice Parameter	String		Lattice parameter of compound
Space Group	String		Space group of compound
Coercivity	Numeric	Oe	Coercivity value of compound
Magnetization	Numeric	A/M	Magnetization value of compound
Magnetic Moment	Numeric	$\mu$ B	Magnetic moment value of compound
Remanence	Numeric	A/M	Remanence value of compound
Susceptibility	Numeric		Susceptibility value of compound
DOI	String		Source of the entire collected information
Experimental	Boolean		Experimental status (Yes/No) of the article

elements in the database are summarized in Figure 2c. Materials containing elements with high Curie temperatures, such as iron (Fe), cobalt (Co), and nickel (Ni), are numerous. Furthermore, some other elements like Mn, La, Sr, Cu, B, Al, Cr, and Ce are also present in appreciable frequencies, which are necessary for the construction of high-performance magnetic materials. Noticeably, this database contains a huge number of magnetic compounds without rare earth elements. It is potentially useful for discovering permanent magnets without rare-earth elements. Figure 2d displays the distribution of compound types in our database. Approximately 40% are ternary compounds (composed of three distinct elements). The remaining compounds are predominantly quaternary, quinary, and binary.

To validate our work, we randomly chose 200 records from our database and manually reviewed the original article associated with these records. The overall precision of the database is 0.97, with details of the validation process provided in the Supplementary Materials.

### Machine Learning Model for Classifying Materials

To classify the materials into non-magnet (NM), ferromagnet(FM), and antiferromagnet(AF) categories, we built a random forest classifier model based on NEMAD database, see details in the Methods section. Non-magnetic materials used to train the model are taken from the Materials Project. A consistent accuracy of 0.9 on both validation and testing sets underpins the strong generalization of our model toward unseen data. We provide detailed performance metrics for every class across the training, validation, and testing datasets in Table 2. Precision, recall, and F1- score for all classes on the validation and testing sets are consistent, demonstrating that the model is not biased towards the specific subset of data. The overall performance of the model is slightly better in the training set than the testing set, indicating minor over-fitting but the model still remains robust. The AFM class has a slightly lower value of performance metrics compared to other classes, which may be attributed to the smaller antiferromagnetic records in our training dataset. This conclusion is supported by the consistent under-performance of the AFM class across validation and testing sets. Figure 3a and 3b present the confusion matrices which further illustrate the classification performance across validation and testing datasets.

Existing classification models in literature usually classify NM, FM, and AFM using two-step approach; the first step is to classify only non-magnetic and magnetic compounds, and only magnetic materials are passed into the second step to classify FM or AFM<sup>30,32</sup>. Our model achieves one-step classification successfully. Besides, almost all of them are trained on the DFT-generated dataset. In contrast, our model was trained on dataset of first hand experimental reports only. It shows that only input of chemical composition is enough to classify the magnetic materials with appreciable accuracy.

Learning how our models use the input features is key to understand their predictions and the relationships in our data. Machine learning models, especially complex ones like neural networks, are notorious for their black boxes nature; and it is hard to see how they are making predictions based on the input features. Figure 3c shows the feature importance score, where the most important features are the average atomic magnetic moment, the average atomic mass, the average atomic electronegativity, and the average atomic number. Other influential features include the presence of Mn, Fe, O, and Co atoms.



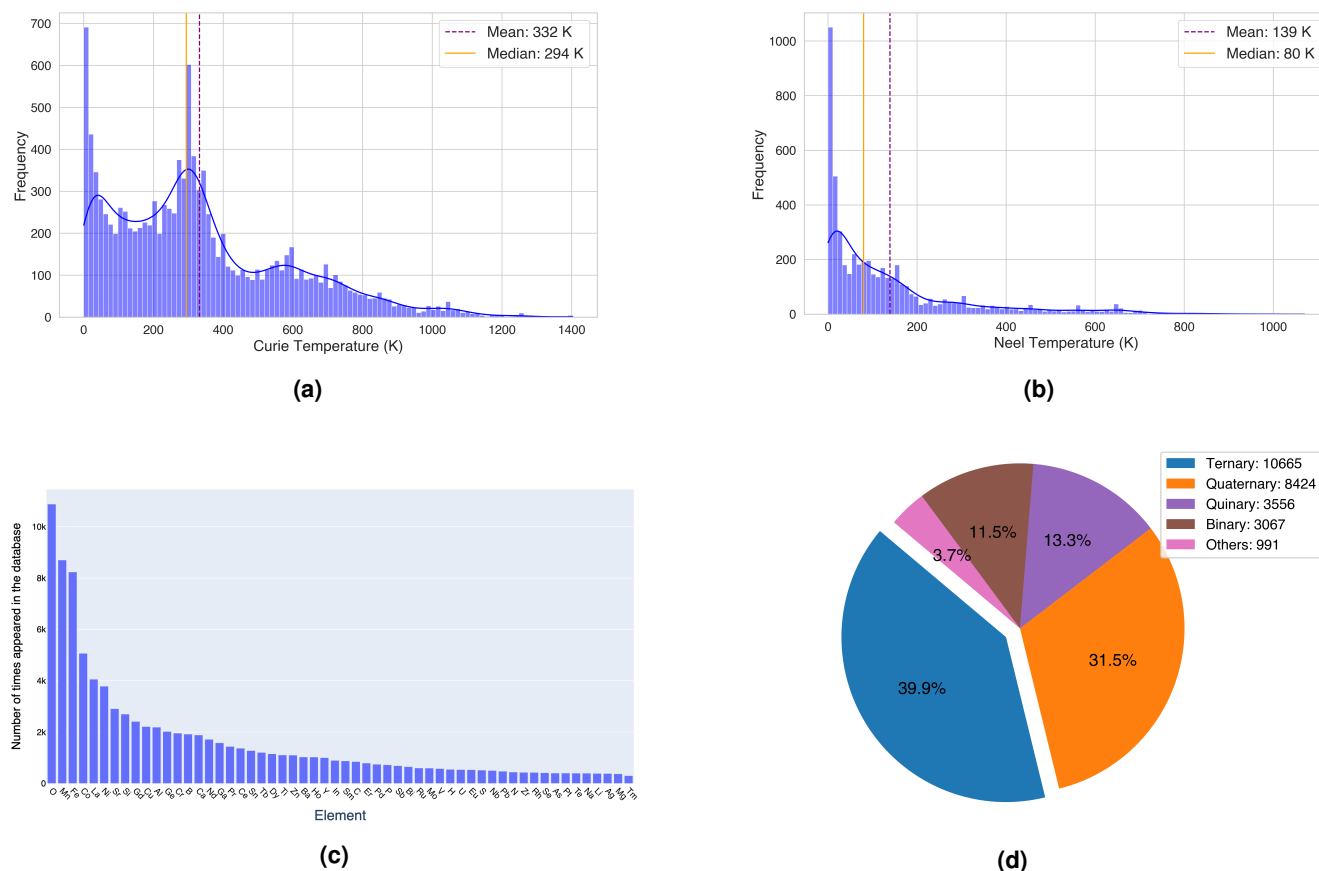


**Figure 2. Comprehensive analysis of the NEMAD database.** Histogram display the distribution and frequencies of the (a) Curie and (b) Néel temperatures across the database. (c) Bar chart represents the frequency of each element present in the database, highlighting the most common elements in magnetic materials. Only elements with a frequency greater than 300 are included. (d) Pie chart categorizes materials into binary, ternary, quaternary, quinary, and higher-order compounds, depicting their relative proportions within the database.

## Regression Model for Predicting Curie Temperature of Ferromagnetic Compounds

In this section, we developed and compared different regression models, including Random Forest (RF) regressor, Extreme Gradient Boosting (XGBoost), and Ensemble Neural Network (ENN), toward accurate prediction of the Curie temperature for a ferromagnetic compound. These Models were trained on two different datasets, one with all the unique ferromagnetic records in the NEMAD database and another with balanced dataset. This balanced dataset was achieved by randomly removing the data points with lower Curie temperature in the NEMAD database to achieve a more uniform temperature distribution. For details on the dataset distribution, see the model development section in the Methods section. Model performance was measured with standard metrics, including R-squared ( $R^2$ ), mean absolute error (MAE), and root mean squared error (RMSE). Furthermore, 5-fold cross-validation was performed to make the results more generic and robust. Table 3 provides detailed performance metrics of these models for test set of each dataset. This implies that across both datasets, the performance of the XGBoost model was greater than that of RF and the ENN model. For the original dataset, the XGBoost model achieved an  $R^2$  value of 0.80, MAE of 66K, and RMSE of 114K, slightly outperforming both RF ( $R^2 = 0.80$ , MAE = 70K, RMSE = 114K) and ENN ( $R^2 = 0.79$ , MAE = 63K, RMSE = 118K). Similarly, for the balanced dataset, the XGBoost model reached an  $R^2$  value of 0.86 MAE of 62K, and RMSE of 105K while RF and ENN attained ( $R^2=0.83$ , MAE = 72K, RMSE = 113K) and ( $R^2=0.84$ , MAE = 65K, RMSE = 110K) respectively. Notably, all models performed better using the balanced dataset; in particular, performance improved most for the XGBoost model. On this balanced dataset, this resulted in a gain of 6% in predictive accuracy for the XGBoost model and 3% and 5% improvement for the RF and ENN model, respectively. Higher performance on the balanced dataset indicates that models are better at capturing the relationships within higher temperature ranges. This could be an improvement due to the increased relative representation of the higher temperature data.

The plots between the predicted and actual Curie temperature for test set of balanced dataset are shown in Figures 4d, 4e,

**Table 2.** Evaluation metrics used to assess the performance and effectiveness of classification model.

Dataset	Class	Precision	Recall	F1-Score	Accuracy
Training (60%)	FM	1.00	1.00	1.00	0.99
	AFM	0.99	0.98	0.99	
	NM	1.00	1.00	1.00	
Validation (20%)	FM	0.92	0.90	0.91	0.90
	AFM	0.81	0.75	0.78	
	NM	0.92	0.97	0.94	
Testing (20%)	FM	0.90	0.90	0.90	0.90
	AFM	0.82	0.76	0.79	
	NM	0.93	0.96	0.94	

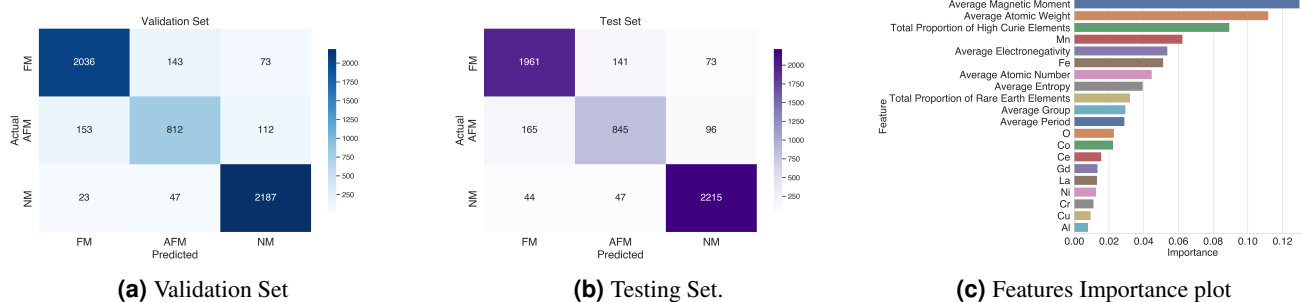


**Figure 3. Performance and analysis of the classification model for magnetic materials.** Confusion matrix illustrates the performance of the classification model on the (a) validation set (b) test set, showing the number of true positive, true negative, false positive, and false negative predictions. (c) The feature importance plot ranks the significance of various features used in the classification model. In the Random Forest model, feature importance scores are computed as the mean and standard deviation of the accumulation of impurity decrease within each tree in the forest. The features are then sorted by these importance scores, and the top 20 most influential features are displayed.

and 4f. This model based on the balanced dataset has better performance than that on the original dataset, as shown in 4a, 4b, and 4c. In the region where the Curie temperature is greater than 500K in the original dataset, all three models underestimated the Curie temperature. This suggests the necessity of expanding the database by adding higher Curie temperature data points in the future.

To further assess the model's predictive accuracy, we conducted an error analysis using the absolute error plots. Figure 4g, 4h, and 4i presents these plots for all three models across balanced dataset. We fitted an exponential curve to each error distribution to characterize the error pattern. In XGBoost and ENN, 63% of the test data have an absolute error of less than 50K, whereas in RF model, this proportion is 55%.

To make the model more understandable we calculated the feature importance by calculating the correlation between the features and the target. Figure 4j, 4k, and 4l shows the feature importance of top 20 features. In all three models, the proportion of Fe atom, magnetic element proportion, rare element proportion, average atomic magnetic moment, and proportion of Co atom are the top predictors.

### Regression Model for Predicting Néel Temperature of Antiferromagnetic Compounds

Similar method can be developed to predict Néel temperatures of the antiferromagnetic compounds. Details of procedures for data cleaning and model building are explained in the Methods section. We developed and evaluated three distinct models: Random Forest (RF) regressor, Ensemble Neural Network (ENN), and XGBoost. ENN and XGBoost demonstrated superior performance, while RF showed comparatively poorer fit. XGBoost achieved the highest performance with an  $R^2$  value of 0.85, followed closely by ENN with an  $R^2$  of 0.82. On the other hand, the RF model lagged behind with an  $R^2$  of 0.76. The MAE and RMSE further demonstrated the performance of the model. The XGBoost model had the lowest error metrics with an MAE of 32K and RMSE of 67K, while ENN showed a little lower accuracy with an MAE of 36K and RMSE of 73K. However, RF showed substantially higher error rates, with an MAE of 44K and RMSE of 83K.

**Table 3.** Evaluation metrics used to assess the performance and effectiveness of various regression models trained on two datasets for predicting Curie temperature.

Model	Dataset	R-squared (Test)	MAE (Test)	RMSE (Test)
Random Forest	Original	0.80	70K	114K
	Balanced	0.83	72K	113K
Ensembled Neural Network	Original	0.79	63K	118K
	Balanced	0.84	64K	110K
XGBoost	Original	0.80	66K	114K
	Balanced	0.86	62K	105K

Figures 5 show the predicted versus actual Néel temperature plot, absolute error plot, and feature importance plot using ENN and XGBoost models. As the figures suggest, the predicted temperatures at the high-temperature region quite deviate from the actual one, this is due to lack of enough training data points in this region. The absolute error plots demonstrate that around 64% data points in the test set have an absolute error of less than 20K for the XGBoost model, whereas in the ENN Model, this proportion is 60%. Feature importance plots show the top 20 most decisive features to predict the Néel temperature of the antiferromagnetic compounds. Both model shows the proportion of Iron(Fe) atom as the most important feature. A significant number of transition metal oxides, including those of iron, manganese, Cobalt, and nickel, exhibit antiferromagnetic behavior. This is due to the superexchange interactions between the magnetic ions mediated by oxygen anions, which often result in anti-parallel alignment of adjacent spins, leading to antiferromagnetic ordering<sup>48,49</sup>. So the appearance of the oxygen atom on both models' importance feature list shows that our models somehow captured the pattern correctly.

### Screening High Performance Magnetic Material from Materials Project Database

With the success of training neural network models presented above, we implement our machine learning models in this section on completely unseen data to screen out novel materials with specific properties. To this end, the Materials Project database was selected, from where marked magnetic materials with features like chemical composition, magnetic phase, and stability were downloaded using an API key. First, we removed materials which are already included in our database. Although every material from the Materials Project has a label of its magnetic state, we still implemented our classification model on the dataset to reconfirm the magnetic state, ie, ferromagnetic, antiferromagnetic, or non-magnetic, of each compound. We listed 602 ferromagnetic and 237 antiferromagnetic compounds having the consensus between our classification results and the Materials Project database. We then used our regression models to predict the Curie and Néel temperature of all the above-listed ferromagnetic and antiferromagnetic compounds. Table 4 lists some potential high Curie temperature ferromagnetic compounds with predicted Curie temperatures greater than 500K for at least two best models, XGBoost and ENN, as well as antiferromagnetic compounds with predicted Néel temperatures greater than 100K for at least the XGBoost model. We have detailed all 62 potential high Curie temperature ferromagnetic compounds and 19 antiferromagnetic compounds in the Supplementary Materials. Future experimental verification of these predictions are strongly encouraged.

**Table 4.** The list of potential high Curie temperature candidates with predicted Curie temperatures and potential AFM compounds with predicted Néel temperature from our three best machine learning models is yet to be verified by experiments. The full list is shown in the Supplementary Materials

Material Composition	Predicted Type	Ensemble NN (K)	XGBoost (K)	RF (K)
VFeCoGe	FM	609	710	729
FeCo2Ge	FM	1051	1068	999
LiFeRh2	FM	636	690	577
AlFeCo2	FM	912	928	907
Ba(FeO2)2	FM	660	659	658
GaFe2Co4Si	FM	1042	1013	1007
Fe3RhN	FM	677	689	625
Fe3PdN	FM	646	673	622
Fe3Co3Si2	FM	1042	939	913
AlFe3C	FM	697	784	669
Ga3Fe4Co8Si	FM	1151	1157	1010
Li2Fe12P7	FM	734	655	643
MnCo2Si	FM	823	991	662
MnCo2Sb	FM	617	691	672
MnCo2Sn	FM	802	798	767
NbAlCo2	FM	770	609	605
MnGaCo2	FM	740	668	648
Mn2GaCo4Ge	FM	804	722	658
MnCo2Ge	FM	767	900	803
TaAlCo2	FM	729	609	516
MnAlCo2	FM	805	757	700
Sr6(CoO3)5	FM	642	746	620
TiFeO3	AFM	60	137	
Sr2FeBrO3	AFM	139	300	
TaFeO4	AFM	53	122	
BaFe2P2O7F2	AFM	132	132	
Cr3(FeO6)2	AFM	136	123	
Lu(Al2Fe)4	AFM	99	125	
Sr2Co(BrO)2	AFM	63	116	
Ba2Mn2Se2OF2	AFM	105	102	
La2Mn2Se2O3	AFM	150	151	

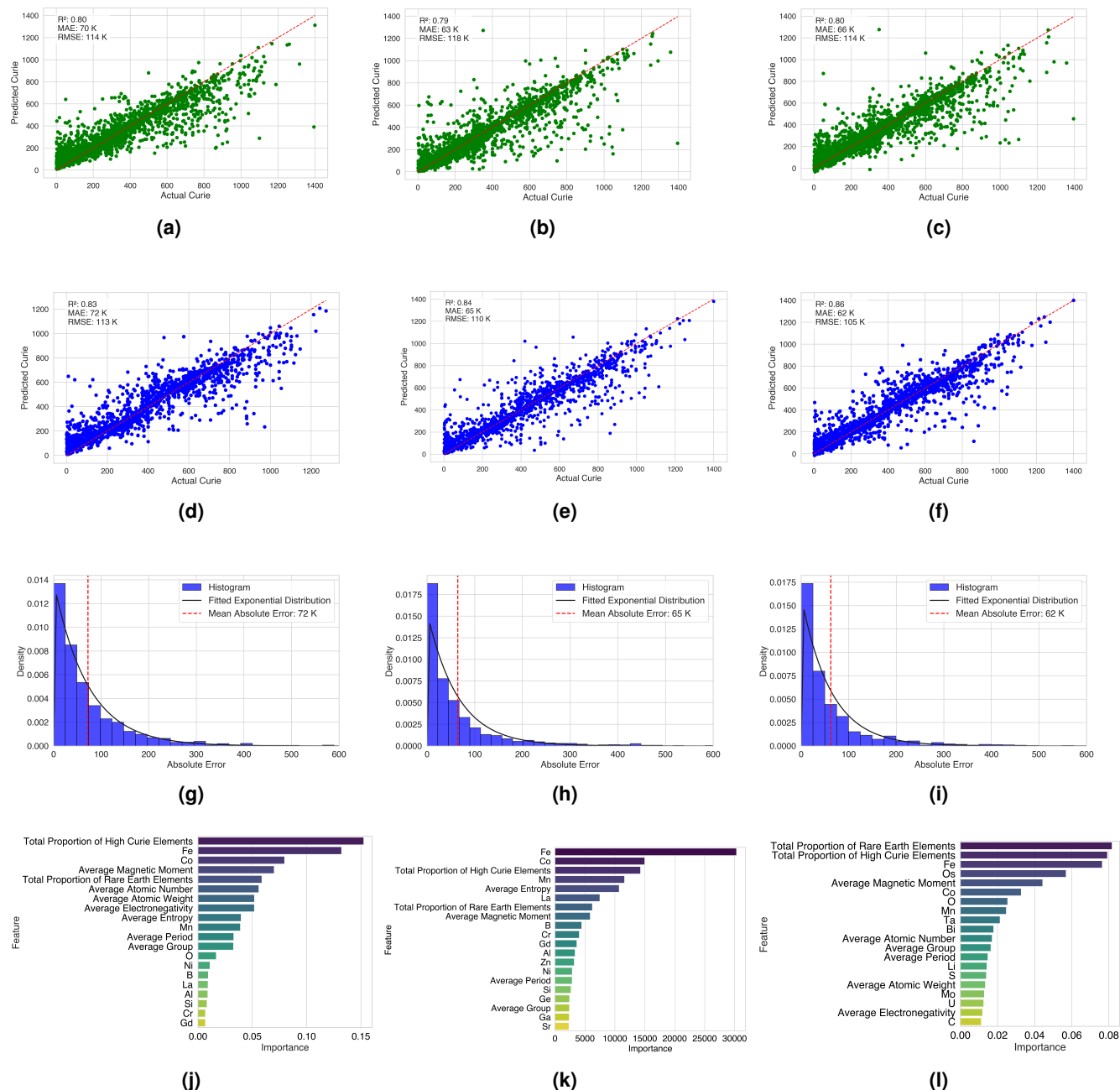
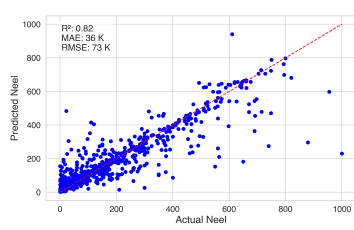
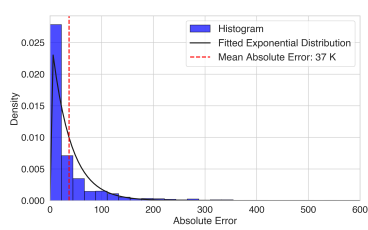


**Figure 4. Comprehensive analysis of Curie temperature prediction models using different datasets and evaluation metrics. (a-c)** Comparison of predicted vs. actual Curie temperatures for the test set of the Original dataset, derived from the NEMAD database. **(d-f)** Similar comparison for the Balanced dataset, where some compounds with Curie temperatures below 300K were randomly removed to achieve a balanced distribution of high and low-temperature compounds. For both datasets, the plots show predictions from three models: Random Forest **(a,d)**, Ensemble Neural Network **(b,e)**, and XGBoost **(c,f)**. Each plot displays the coefficient of determination ( $R^2$ ), mean absolute error (MAE), and root mean square error (RMSE) in the top left corner. **(g-i)** Absolute error distribution and exponential fit across different models for the test set of the Balanced dataset: **(g)** Random Forest, **(h)** Ensemble Neural Network, and **(i)** XGBoost. **(j-l)** Feature importance plots for Curie temperature prediction models trained on the Balanced dataset, highlighting the top 20 features crucial for accurate predictions: **(j)** Random Forest, **(k)** Ensemble Neural Network, and **(l)** XGBoost. All models utilized features generated from chemical compositions to make predictions. This comprehensive visualization allows for a direct comparison of model performance across different datasets, error distributions, and feature importances, providing insights into the strengths and characteristics of each predictive model in the context of Curie temperature prediction.

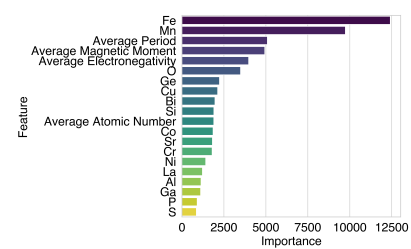




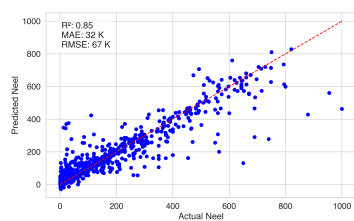
(a)



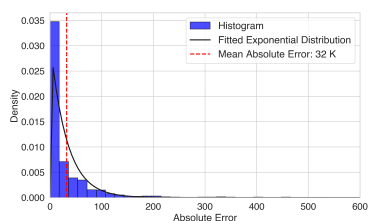
(b)



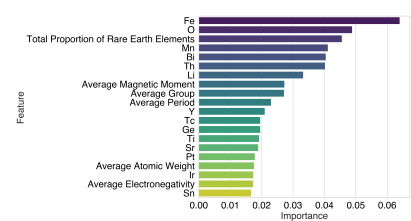
(c)



(d)



(e)



(f)

**Figure 5. Evaluation of Ensemble Neural Network and XGBoost models for Néel temperature prediction using features generated from chemical compositions. (a-c) Ensemble Neural Network model results: (a) Predicted vs. actual Néel temperature for the test set, (b) Absolute error distribution, (c) Feature importance plot. (d-f) XGBoost model results: (d) Predicted vs. actual Néel temperature for the test set, (e) Absolute error distribution, (f) Feature importance plot.**

## Discussion

It is interesting to note that our database only includes 35% antiferromagnetic materials, far less than ferromagnets. One reason may be because of the presence of many ferromagnetic alloys in the database. The number of alloys is in principle unbounded and those containing magnetic elements such as iron are more likely to be ferromagnetic due to their itinerancy nature. On the other hand, there exist many antiferromagnets in transition metal oxides. Experimental reports for this community were published in journals outside of Elsevier. It is thus important to expand the coverage of articles to include other publishers such as the American Physical Society. A large database on magnetic materials is expected.

A key product of this study is the development of a user-friendly website [www.nemad.org](http://www.nemad.org) that hosts the NEMAD database. This website systematically organizes all the materials, allowing users to easily access detailed information about each material's properties. Users can explore the database and retrieve material data directly from the platform. We will continue to increase our database size.

Our database also include the structural information of magnetic materials. This can be used in building a more powerful models, such as the graph neural network, in predicting magnetic properties. We also built a simple XGBoost machine learning model to incorporate these structure features like crystal system and space group (detailed included in the Supplementary Materials). The XGBoost model achieved an  $R^2$  value of 0.86, MAE of 52K, and a RMSE of 89K. The MAE and RMSE values are slightly improved compared to the model without structural information.

Our LLM-based approach of extracting information and creating automated databases is versatile and can be applied to other areas of material science, such as superconducting, thermoelectric, photovoltaic, ferroelectric materials, etc. This method has the potential to transform how we gather and use scientific knowledge. The method used here to build the predictive models can also be adapted to predict other critical properties of magnetic materials, such as coercivity and saturation magnetization.

In summary, this study presents an effective method for discovering high-performance magnetic materials using large language models and machine learning techniques. A comprehensive database of magnetic materials was built. It includes not only the chemical and magnetic information, but also structural information. The machine learning models trained based on this database can be used to accurate prediction of new magnetic materials. These tools can be employed by researchers to develop next-generation magnetic materials through large-scale materials screening .

## METHODS

### Database Compilation

Figure 6 illustrates the detailed workflow of the method used in this work. We began by compiling a comprehensive list of 40,000 Digital Object Identifiers (DOIs) of scientific articles related to Magnetic Materials by searching relevant keywords (Ferromagnetic, Anti-ferromagnetic, Curie, and Néel) and deploying web scraping tool in various journal websites. We downloaded the article for all listed DOIs using the authenticated API request. These articles were primarily obtained in XML format, which often contains a hierarchical structure with nested elements. We developed a custom XML parsing script to extract the full content of articles, including tabular data, from pre-downloaded XML-formatted documents. The script converts all unstructured textual and tabular information into plain text format and then saves it as a CSV file with the following features.

- DOI
- Title
- Abstract
- Description (body part of the article)

GPTArticleExtractor<sup>47</sup> method provides a way to make a comprehensive material property database by automatically extracting data from scientific articles with high precision and recalls. This method leverages the cutting edge Large Language Models like GPT-3.5 by incorporating the OpenAI API key. One can extract their desired information from articles by just modifying the prompts used in the workflow. So effective prompts are crucial for the accuracy and efficiency of this method.

For this study, we listed the desired properties to extract from articles, including material chemical composition, magnetic phase transition temperatures (Curie, Néel, and Curie-Weiss), structural information (Crystal Structure, Lattice Structure, Lattice Parameters, and Space Group), and magnetic properties (Coercivity, Magnetization, Magnetic Moment, Remanence, and Susceptibility). We carefully reviewed literature from a range of publications to comprehend the trends and writing styles associated with these attributes to create effective prompts. We formulated the question prompts to extract the custom need information. For instance, to extract material chemical composition, we formulated the prompt like this " Provide an exact chemical composition of the magnetic materials studied in the article, some materials' composition are expressed with the variable proportion of elements. So include any value of the variable mentioned."

Large Language Models are not still free from the limitation of the input tokens. It is less effective if we use the entire sections of the paper as an input of these models. To include only information related to the question prompt in the input, GPTArticleExtractor tokenized the articles by segmenting the text into chunks of 500 tokens each. Following that, these segments were examined in a vector space to determine word similarity using metrics like Euclidean distance. By comparing the vectorized text segments with particular question prompts, the model figured out the five most relevant segments using Facebook AI Similarity Search (FAISS)<sup>50</sup>. This method allowed us to focus on the most relevant information, improving answer quality while minimizing input tokens and computing expenses. After selecting the most correlated information from the articles, it generates the output with desired properties by utilizing the summarization prompt. To ensure consistency in output results, we employed one-shot prompting where the prompt included an example output format. This technique enabled the generation of accurate and structured output data.

Although this workflow performs well for handling longer articles with the help of GPT 3.5 and GPT 4 models, it still has certain shortcomings. The relevant segment parts occasionally missed important materials and properties information when multiple entries were present in a single article and struggled to extract stoichiometric ratios presented in variable forms. We modified this workflow with the advent of the powerful GPT-4o model. We included all the details of the article except the introduction and reference sections as input in the modified workflow. This all-inclusive strategy performed better than the prior technique, producing outputs that were more comprehensive, precise, and organized. This approach managed various material compositions and properties present in a single article by accurately creating lists of dictionaries, where each entry includes all the information associated with a single chemical composition. Some chemical compositions extracted by our model missed certain properties. Therefore, we established a rule for including these materials in the database: a chemical composition must contain at least phase transition temperature information to be included. Finally, We built the automated database of magnetic materials with 26,706 entries.

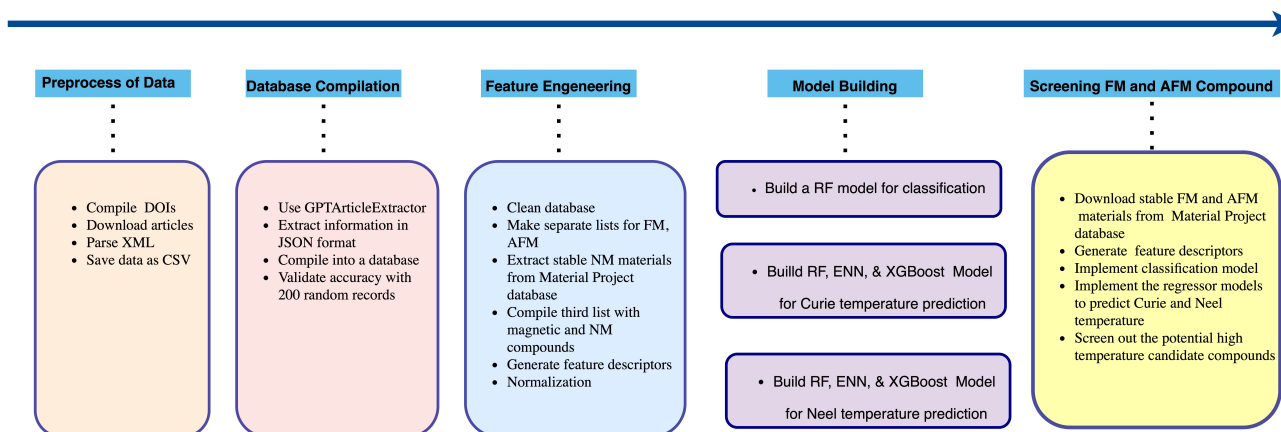


**Figure 6. Detailed workflow for high-performance magnetic material discovery.** The workflow is divided into key stages, each represented by a block containing brief bullet points summarizing the methods and techniques employed. These blocks detail the sequential steps from DOIs compilation to materials screening, illustrating the comprehensive approach taken to screen high-performance magnetic materials.

## Feature Engineering

A feature is the numerical representation of data used as input for the model. They are represented in the multi-dimensional space as vectors,  $X = (x_1, x_2, \dots, x_n) \in \mathbb{R}^n$ . It encapsulates all central aspects of data that are relevant to the target variable. Feature engineering generates the most appropriate features based on the specific data, model, and task. This is generally one of the critical steps in developing a predictive model, as it dictates how well and effectively such a model can perform. The importance of feature engineering is more prominent in materials science, where the relationships among material composition, structure, and properties are complex. Proper feature engineering in this domain thus calls for a delicate balance between domain expertise and data-driven insight in order to effectively capture the underlying physics and chemistry regulating the behavior of materials.

In this study, we have focused more on the chemical composition and structural properties to make a feature vector. From the chemical formula, we built up an elemental proportion vector for each compound that might represent the compositional complexity of materials. This vector gives a proportional indication of how each element is distributed in a material's chemical composition. First, we counted the total number of unique elements found in all the compounds in the dataset. In this case, we

found 84 unique elements, which cover a big part of the periodic table. Then we generated an 84-dimensional vector for each compound where each component corresponds to one specific element. The elemental proportion  $p_i$  for element  $i$  is defined as:

$$p_i = \frac{n_i}{N} \quad (1)$$

where  $n_i$  is the number of atoms of element  $i$  in the compound, and  $N$  is the total number of atoms in the compound. Thus, our elemental proportion vector is represented as:

$$p = (p_1, p_2, p_3, \dots, p_{84}) \quad (2)$$

where  $p_i$  take zero value if the element is not present in the material chemical composition. We have also generated other features related to material using atomic properties. For example, we constructed the average atomic number of each compound with the atomic number of every element in it. We did this computation by summing all products of elemental proportion vectors with atomic numbers of corresponding vectors. Mathematically,

$$\text{Average Atomic Number}(\bar{Z}) = \sum_{i=1}^{84} p_i Z_i \quad (3)$$

where  $p_i$  is the proportion of element  $i$  in the compound and  $Z_i$  is the atomic number of element  $i$ . Similarly, we generated several additional features like average atomic weight, average electronegativity, average magnetic moment, average group, and average period of all compounds in the dataset<sup>51</sup>.

Additionally, we calculated the L2 stoichiometry norm and Entropy from the chemical composition of the compound. We used the following formulas to calculate these features<sup>52,53</sup>.

$$\text{L2 Stoichiometry Norm (L2)} = \sqrt{\sum_{i=1}^{84} p_i^2} \quad (4)$$

$$\text{Entropy}(\bar{S}) = -\sum_{i=1}^{84} p_i \log p_i \quad (5)$$

The last two features from the chemical composition are the total proportion of high Curie temperature magnetic elements like Fe, Co, and Ni, and a total proportion of the rare earth elements in the compound.

For the structure-informed model, we created two additional features from the structural details. We constructed a crystal system feature for compounds for which the crystal system is available. There exist seven crystal systems, and so this categorical feature was numerically encoded by assigning a different number from 1 to 7 for each of them. From the space groups of the compounds, we then generated the space group feature. There are 230 space groups, and we transform this categorical feature into a numerical representation by assigning different integer numbers between 1 and 230 for each unique space group. Information on the space group provides information about the symmetry of a crystal and its atomic arrangement, which could be useful for the prediction of magnetic transition temperatures or any other magnetic properties. All features along with their corresponding dimensions are provided in the Supplementary Materials.

### Model Development: Classification Model

To classify the materials as nonmagnetic (NM), ferromagnetic (FM), or antiferromagnetic (AFM), we used the random forest classifier. Random Forest is an ensemble learning method that constructs many decision trees during training and generates the class that is a mode of the classes of the individual trees. It is robust against over-fitting and capable of handling high-dimensional feature spaces.

Our database contains only magnetic materials, so it is impossible to make a model only with our data set to classify magnetic and nonmagnetic materials. We took 11,389 stable non-magnetic materials from the Material Project Database<sup>10</sup> and combined them with our database, resulting in 28,168 unique entries for model development. We generated features from chemical composition, as explained in the feature engineering section. We constructed a target feature with available material type information. Since there are three types of materials, we encode this categorical feature numerically by assigning a unique number from 1 to 3 to each material type. Using the Scikit-learn library<sup>54</sup>, we randomly divided the dataset into three mutually exclusive partitions: 60% for training, 20% for validation, and the remaining 20% for testing purposes. Most

machine learning models include one or more hyperparameters, which cannot be learned from the data and therefore need to be specified beforehand. We specified different sets of hyperparameters in the models, and the validation set later determined the best-performing set. A random forest classifier model was trained, and a five-fold cross-validation technique was used to find the best-performing hyperparameters by initializing GridSearchCV. We then tested our trained model on test set data. The best-performing hyperparameters are as follows: [Number of estimators: 500, Maximum depth: None, Maximum samples split: 2, Minimum samples leaf: 1, Maximum features: sqrt]

### Model Development: Regression Models

In this section, we built several machine learning models such as random forest (RF) regressors, ensemble neural networks (ENN), and extreme gradient boosting (XGBoost) to estimate the Curie and Néel temperatures of corresponding ferromagnetic and antiferromagnetic materials. First, we made a different dataset for both ferromagnetic and anti-ferromagnetic compounds. We have collected compounds from our NEMAD database. A ferromagnetic dataset includes 11923 compounds with different chemical compositions, and an anti-ferromagnetic dataset contains 5389 unique compounds. The distribution of data in the ferromagnetic dataset is not uniform. We have almost 51% of the total compounds with Curie temperature lower than 300K and 22% of the total compounds with Curie temperature greater than 600K. We believe the dataset with this distribution is less appropriate for accurately predicting high Curie temperatures. We created a balanced dataset to address this issue by randomly removing some entries with Curie temperature values lower than 300K. The balanced dataset contains 8249 unique compounds. We then created another data set for the structure-informed model of ferromagnetic compounds. This dataset contains 5,176 entries with additional features like crystal system and space group. Then, we selected the features and targets for the machine learning models. For the Curie temperature prediction model, the target is the value of the Curie temperature, while for the Néel temperature prediction model, the target is the value of the Néel temperature. Both targets contain values in different units. We converted all temperature records to the Kelvin scale. Some of the compounds contain temperatures in a certain range. To get a single value, we took a mean of the two numbers: the initial and final numbers in the range.

Using the Scikit-learn library, we built machine learning models for all datasets mentioned above: the original dataset, balanced dataset, and structure including datasets of ferromagnetic compounds and a dataset of antiferromagnetic compounds. We built a Random Forest model with a 60/20/20 split for training, validation, and testing. The model's performance was optimized using five-fold cross-validation with the following hyperparameters: [Number of estimators: 1000, Maximum depth: None, samples split: 2, samples leaf: 1, Maximum features: sqrt]. Similarly, we built an XGBoost model with the following hyperparameter: [Number of estimators: 500, Maximum depth: 12, Learning rate: 0.08, Subsample: 0.8, Column sample by tree: 0.6]

We created an ensemble of 30 fully connected neural networks, each with 8 hidden layers. We provided the same input features as fed into the RF and XGBoost models to the input layers of each network. We used the ReLU activation function and the Adam optimizer with a learning rate of 0.001 for all networks. The model was trained on 80% of the dataset, and the remaining 20% was used for testing purposes. The final prediction was the average output from all 30 networks, which outperformed a single neural network.

### Evaluation Metrics

For the evaluation of the classification model, we used four metrics such as precision, recall, f1-score of each class of materials and the accuracy of a model<sup>55</sup>.

- Precision quantifies the degree of accuracy of the model's positive predictions. For each class, it's the ratio between correct prediction and all instances predicted to belong to that class. High accuracy implies that the model has a low false positive rate. Mathematically,

$$\text{Precision}_i = \frac{\text{True Positive (TP)}_i}{\text{True Positive (TP)}_i + \text{False Positive (FP)}_i} \quad (6)$$

- The model's recall, a key measure, quantifies its capacity to identify every good case. For each class, recall is the ratio between correct predictions and all actual instances of that class. High recall implies that the model has a low false negative rate. Mathematically,

$$\text{Recall}_i = \frac{\text{True Positive (TP)}_i}{\text{True Positive (TP)}_i + \text{False Negative (FN)}_i} \quad (7)$$

- The F1-score is calculated by taking the harmonic mean of precision and recall. It should balance both metrics in principle. It is useful for unevenly distributed classes. A high F1 score usually indicates that the model performs very



well in terms of both precision and recall. Mathematically,

$$\text{F1-Score}_i = \frac{2 * \text{Precision}_i * \text{Recall}_i}{\text{Precision}_i + \text{Recall}_i} \quad (8)$$

- Accuracy is the ratio between correct predictions (TP and TN) among the total number of cases classified. It gives an overall estimate of how often the model is correct across all classes. Mathematically,

$$\text{Accuracy} = \frac{\text{Correct Predictions}}{\text{Total Predictions}} \quad (9)$$

For the evaluation of the regression model, we used three metrics such as coefficient of determination ( $R^2$ ), mean absolute error (MAE), and root mean square Error (RMSE).

- $R^2$  assesses how effectively a machine learning model explains variance in the target variable compared to a simple mean model. The value ranges from 0 to 1, and higher values generally indicate better fits of the model. Mathematically,

$$R^2 = 1 - \frac{\sum_{j=1}^n (y_j - \hat{y}_j)^2}{\sum_{j=1}^n (y_j - \bar{y})^2} \quad (10)$$

where  $y_j$ ,  $\hat{y}_j$  and  $\bar{y}$  are the actual value, predicted value and mean of the actual value.

- MAE is the average of the absolute differences between predictions and actual values. It gives an idea of how far the predictions are from the actual values on average. Lower MAE values indicates better model performance.

$$\text{MAE} = \frac{1}{n} \sum_{j=1}^n |y_j - \hat{y}_j| \quad (11)$$

- RMSE measures the standard deviation of the residuals or simply prediction errors. Lower RMSE value indicate better model performance. RMSE gives a relatively high weight to large errors, which means it's more sensitive to outliers than MAE.

$$\text{RMSE} = \sqrt{\frac{1}{n} \sum_{j=1}^n (y_j - \hat{y}_j)^2} \quad (12)$$

## Acknowledgements (not compulsory)

This work was supported by the Office of Basic Energy Sciences, Division of Materials Sciences and Engineering, U.S. Department of Energy, under Award No. DE-SC0020221.

## Author contributions statement

J.Z. conceived the project. S.I. and Y.Z. built the materials database using LLMs. S.I. developed classification and regression models for materials prediction. Y.Z. developed the NEMAD website. S.I., Y.Z. and J.Z. wrote the manuscript.

## Additional information

To include, in this order: **Accession codes** (where applicable); **Competing interests** (mandatory statement).

The corresponding author is responsible for submitting a [competing interests statement](#) on behalf of all authors of the paper. This statement must be included in the submitted article file.

## References

1. Coey, J. M. *Magnetism and magnetic materials* (Cambridge university press, 2010).
2. Gutfleisch, O. *et al.* Magnetic materials and devices for the 21st century: stronger, lighter, and more energy efficient. *Adv. materials* **23**, 821–842 (2011).
3. Jungwirth, T. *et al.* The multiple directions of antiferromagnetic spintronics. *Nat. Phys.* **14**, 200–203 (2018).

4. Skokov, K. P. & Gutfleisch, O. Heavy rare earth free, free rare earth and rare earth free magnets-vision and reality. *Scripta Materialia* **154**, 289–294 (2018).
5. Coey, J. Permanent magnetism. *Solid State Commun.* **102**, 101–105 (1997).
6. Coey, J. Perspective and prospects for rare earth permanent magnets. *Engineering* **6**, 119–131 (2020).
7. Himanen, L., Geurts, A., Foster, A. S. & Rinke, P. Data-driven materials science: status, challenges, and perspectives. *Adv. Sci.* **6**, 1900808 (2019).
8. Kohn, W. & Sham, L. J. Self-consistent equations including exchange and correlation effects. *Phys. review* **140**, A1133 (1965).
9. Jain, A., Shin, Y. & Persson, K. A. Computational predictions of energy materials using density functional theory. *Nat. Rev. Mater.* **1**, 1–13 (2016).
10. Jain, A. *et al.* Commentary: The materials project: A materials genome approach to accelerating materials innovation. *APL materials* **1** (2013).
11. Curtarolo, S. *et al.* Aflow: An automatic framework for high-throughput materials discovery. *Comput. Mater. Sci.* **58**, 218–226 (2012).
12. Curtarolo, S. *et al.* Aflowlib.org: A distributed materials properties repository from high-throughput ab initio calculations. *Comput. Mater. Sci.* **58**, 227–235 (2012).
13. Saal, J. E., Kirklin, S., Aykol, M., Meredig, B. & Wolverton, C. Materials design and discovery with high-throughput density functional theory: the open quantum materials database (oqmd). *Jom* **65**, 1501–1509 (2013).
14. Illas, F., Moreira, I. d. P., Bofill, J. M. & Filatov, M. Spin symmetry requirements in density functional theory: the proper way to predict magnetic coupling constants in molecules and solids. *Theor. Chem. Accounts* **116**, 587–597 (2006).
15. Mimura, Y., Imamura, N., Kobayashi, T., Okada, A. & Kushiroya, Y. Magnetic properties of amorphous alloy films of fe with gd, tb, dy, ho, or er. *J. Appl. Phys.* **49**, 1208–1215 (1978).
16. Yano, K. Molecular field analysis for melt-spun amorphous fe<sub>100-x</sub>gd<sub>x</sub> alloys (18 ≤ x ≤ 60). *J. magnetism magnetic materials* **208**, 207–216 (2000).
17. Gangulee, A. & Koblik, R. Mean field analysis of the magnetic properties of amorphous transition-metal–rare-earth alloys. *J. Appl. Phys.* **49**, 4896–4901 (1978).
18. Turek, I., Ruzs, J. & Diviš, M. Electronic structure and volume magnetostriction of rare-earth metals and compounds. *J. magnetism magnetic materials* **290**, 357–363 (2005).
19. Turek, I., Kudrnovský, J., Drchal, V. & Bruno, P. Exchange interactions, spin waves, and transition temperatures in itinerant magnets. *Philos. Mag.* **86**, 1713–1752 (2006).
20. Schuch, N. & Verstraete, F. Computational complexity of interacting electrons and fundamental limitations of density functional theory. *Nat. physics* **5**, 732–735 (2009).
21. Cohen, A. J., Mori-Sánchez, P. & Yang, W. Insights into current limitations of density functional theory. *Science* **321**, 792–794 (2008).
22. Butler, K. T., Davies, D. W., Cartwright, H., Isayev, O. & Walsh, A. Machine learning for molecular and materials science. *Nature* **559**, 547–555 (2018).
23. Ramprasad, R., Batra, R., Piliya, G., Mannodi-Kanakkithodi, A. & Kim, C. Machine learning in materials informatics: recent applications and prospects. *npj Comput. Mater.* **3**, 54 (2017).
24. Badini, S., Regondi, S. & Pugliese, R. Unleashing the power of artificial intelligence in materials design. *Materials* **16**, 5927 (2023).
25. Spear, A. D., Kalidindi, S. R., Meredig, B., Kotsos, A. & Le Graverend, J.-B. Data-driven materials investigations: the next frontier in understanding and predicting fatigue behavior. *Jom* **70**, 1143–1146 (2018).
26. Nelson, J. & Sanvito, S. Predicting the curie temperature of ferromagnets using machine learning. *Phys. Rev. Mater.* **3**, 104405 (2019).
27. Court, C. J. & Cole, J. M. Magnetic and superconducting phase diagrams and transition temperatures predicted using text mining and machine learning. *npj Comput. Mater.* **6**, 18 (2020).
28. Singh, P., Del Rose, T., Palasyuk, A. & Mudryk, Y. Physics-informed machine-learning prediction of curie temperatures and its promise for guiding the discovery of functional magnetic materials. *Chem. Mater.* **35**, 6304–6312 (2023).

29. Acosta, C. M., Ogoshi, E., Souza, J. A. & Dalpian, G. M. Machine learning study of the magnetic ordering in 2d materials. *ACS Appl. Mater. & Interfaces* **14**, 9418–9432 (2022).
30. Long, T., Fortunato, N. M., Zhang, Y., Gutfleisch, O. & Zhang, H. An accelerating approach of designing ferromagnetic materials via machine learning modeling of magnetic ground state and curie temperature. *Mater. Res. Lett.* **9**, 169–174 (2021).
31. Belot, J. F., Taufour, V., Sanvito, S. & Hart, G. L. Machine learning predictions of high-curie-temperature materials. *Appl. Phys. Lett.* **123** (2023).
32. Lu, S., Zhou, Q., Guo, Y. & Wang, J. On-the-fly interpretable machine learning for rapid discovery of two-dimensional ferromagnets with high curie temperature. *Chem* **8**, 769–783 (2022).
33. Nguyen, D.-N. *et al.* A regression-based model evaluation of the curie temperature of transition-metal rare-earth compounds. In *Journal of Physics: Conference Series*, vol. 1290, 012009 (IOP Publishing, 2019).
34. Choudhary, A. K. *et al.* Machine learning-based curie temperature prediction for magnetic 14: 2: 1 phases. *AIP Adv.* **13** (2023).
35. Bhandari, C., Nop, G. & Paudyal, D. Accurate prediction of magnetic properties of permanent magnets using machine learning. *Bull. Am. Phys. Soc.* (2024).
36. Gallego, S. V. *et al.* Magndata: towards a database of magnetic structures. i. the commensurate case. *J. Appl. Crystallogr.* **49**, 1750–1776 (2016).
37. Gallego, S. V. *et al.* Magndata: towards a database of magnetic structures. ii. the incommensurate case. *J. Appl. Crystallogr.* **49**, 1941–1956 (2016).
38. Xu, Y., Yamazaki, M. & Villars, P. Inorganic materials database for exploring the nature of material. *Jpn. J. Appl. Phys.* **50**, 11RH02 (2011).
39. Connolly, T. F. *Bibliography of magnetic materials and tabulation of magnetic transition temperatures* (Springer Science & Business Media, 2012).
40. Buschow, K. J. *Handbook of magnetic materials* (Elsevier, 2003).
41. Court, C. J. & Cole, J. M. Auto-generated materials database of curie and néel temperatures via semi-supervised relationship extraction. *Sci. data* **5**, 1–12 (2018).
42. Gilligan, L. P., Cobelli, M., Taufour, V. & Sanvito, S. A rule-free workflow for the automated generation of databases from scientific literature. *npj Comput. Mater.* **9**, 222 (2023).
43. Blundell, S. *Magnetism in condensed matter* (OUP Oxford, 2001).
44. Dagdelen, J. *et al.* Structured information extraction from scientific text with large language models. *Nat. Commun.* **15**, 1418 (2024).
45. Polak, M. P. & Morgan, D. Extracting accurate materials data from research papers with conversational language models and prompt engineering. *Nat. Commun.* **15**, 1569 (2024).
46. Yuan, J., Yang, R., Patra, L. & Liao, B. Enhancing magnetocaloric material discovery: A machine learning approach using an autogenerated database by large language models. *arXiv preprint arXiv:2403.02553* (2024).
47. Zhang, Y. *et al.* Gptarticleextractor: An automated workflow for magnetic material database construction. *J. Magn. Magn. Mater.* **597**, 172001 (2024).
48. Coey, J. Magnetic oxides and other compounds. In *Handbook of Magnetism and Magnetic Materials*, 847–922 (Springer, 2021).
49. Oleś, A. M. Magnetic interactions in transition metal oxides with orbital degrees of freedom. In *AIP Conference Proceedings*, vol. 695, 176–187 (American Institute of Physics, 2003).
50. Johnson, J., Douze, M. & Jégou, H. Billion-scale similarity search with gpus. *IEEE Transactions on Big Data* **7**, 535–547 (2019).
51. Ong, S. P. *et al.* Python materials genomics (pymatgen): A robust, open-source python library for materials analysis. *Comput. Mater. Sci.* **68**, 314–319 (2013).
52. Ward, L., Agrawal, A., Choudhary, A. & Wolverton, C. A general-purpose machine learning framework for predicting properties of inorganic materials. *npj Comput. Mater.* **2**, 1–7 (2016).

53. Troparevsky, M. C., Morris, J. R., Kent, P. R., Lupini, A. R. & Stocks, G. M. Criteria for predicting the formation of single-phase high-entropy alloys. *Phys. Rev. X* **5**, 011041 (2015).
54. Pedregosa, F. *et al.* Scikit-learn: Machine learning in python. *J. machine Learn. research* **12**, 2825–2830 (2011).
55. Sokolova, M. & Lapalme, G. A systematic analysis of performance measures for classification tasks. *Inf. processing & management* **45**, 427–437 (2009).